Contribution from the Department of Chemistry,
University of Arkansas, Fayetteville, Arkansas 72701

Semiempirical Calculation of Iron–Oxygen Interactions

GEORGE BLYHOLDER,* JOHN HEAD, and FERNANDO RUETTE

A modified MINDO procedure works well to discuss iron–oxygen interactions. To our knowledge this is the first application of MINDO to transition-metal compounds. The iron orbitals that contribute most to bonding in FeO are the 4s and 4p orbitals with relatively little contribution from the 3d orbitals. The molecular orbital model used gave a good account of the vibrational frequencies in the various charged species. A rigid molecular orbital model for FeO$^+$ and FeO$^-$ derived from the MO's for FeO was found to have some predictive value, but explicit calculations for FeO$^+$ and FeO$^-$ reveal variations from the predictions. Comparison of calculations for side-bonded and linear FeO$_2$ show that as positive charge on the Fe atom is increased, the linear structure is favored. Back-donation of charge from the Fe atoms into π^* orbitals on oxygen weakens the O–O bond in coordinated O$_2$. No activation barrier is found for rotation of the O–O group from the side-bonded to the linear position. The most stable bond angle in O–Fe–O is calculated to be 180°. For dissociation of the O–O bond in side-bonded FeO$_2$ to form O–Fe–O, an activation energy of 100 kcal/mol is calculated. Negative charge on the complex decreases the activation energy while positive charge increases it.

1. Introduction

The purpose of this paper is to present semiempirical molecular orbital calculations describing the stability and bonding in FeO, FeO$_2$, and OFeO as a function of the charge and geometry. The interaction of oxygen with Fe atoms is of interest because of its bearing on such diverse processes as corrosion of structural metals and oxygen transport in biological systems. There have been a number of reports on the kinetics and the surface-phase structure produced in the early stages of the interaction between a pure iron surface and oxygen.[1-8] Recent detailed examination of the kinetics of the O$_2$ interaction have led to the suggestion of molecularly adsorbed O$_2$ as a precursor state to dissociation into immobile adsorbed oxygen atoms.[7,8] The nature of the adsorbed O$_2$ precursor state or the nature of the sites required to dissociate O$_2$, if indeed there are any requirements for O$_2$ dissociation, have not been discussed.

The interaction of oxygen with Fe atoms coordinated in biological systems has been the subject of several studies.[9-13] Infrared and Raman spectra have been interpreted[11,13] as indicating the O$_2$ is end bonded, as opposed to side bonded, to Fe atoms in +2 or +3 oxidation states. Both ab initio[14,15] and extended Hückel[16,17] calculations have appeared for iron porphyrins and iron porphyrin models. These results favor an end-bonded bent structure over a side-bonded structure, a low spin state, and a close to neutral bonded O$_2$ species that is either slightly positive or negative although one calculation[17] gave bound O$_2$ a charge of 0.56–. Experimental data is interpreted[18] as indicating a negative charge on the bound O$_2$.

In contrast to these iron biological systems, a general review[19] of dioxygen in inorganic coordination complexes reveals an overwhelming preference for a side-bonded structure. For isolated iron atoms in an argon matrix one study[20] has suggested a side-bonded interaction for O$_2$. The reasons for Fe atoms behaving differently from Fe in iron(II) porphyrin and hemerythrin is not clear.

A variety of extended Hückel, CNDO (complete neglect of differential overlap), and INDO methods have been applied to many organic and inorganic molecules and more recently to systems with transition metals.[21-23] In dealing with organic molecules it has been noted that CNDO/2 usually provides a poor estimate of total heats of formation.[24] Of the various semiempirical methods the MINDO procedure[25] appears to offer great potential[24,26] and so was chosen for this study.

2. Calculational Procedure

In the modification of MINDO used here all bonds in which both atoms have an atomic number less than 19 are treated as in MINDO/3. For the one-electron part of the off-diagonal Fock matrix elements involving an orbital on a transition-metal atom the value is modified to be proportional to $3S/R$ rather than just S. Provision is made for the proportionality constant β for a "p" to be different from β for an "s" orbital while β for "d" orbitals is the same as for "s" orbitals. This was done most conveniently for the case where A is a transition metal by use of the equation

$$\beta_p^{AB} = K_p^A \beta_s^{AB}$$

These equations maintain rotational invariance. The repulsive energy is given by the Dewar formula $\gamma + (1/R - \gamma)\alpha e^{-R}$,

(1) (a) M. A. H. Lanyon and B. M. W. Trapnell, *Proc. R. Soc. London, Ser. A*, **227**, 387 (1955); (b) M. W. Roberts, *Trans. Faraday Soc.*, **57**, 99 (1961).
(2) J. Kruger and H. T. Yolken, *Corrosion (Houston)*, **20**, 296 (1964).
(3) S. Chang and W. H. Wade, *J. Phys. Chem.*, **74**, 2484 (1970).
(4) A. J. Pignocco and G. E. Pellissier, *Surf. Sci.*, **7**, 261 (1967).
(5) P. B. Sewell, D. F. Mitchell, and M. Cohen, *Surf. Sci.*, **33**, 535 (1972).
(6) C. Leygraf and S. Ekelund, *Surf. Sci.*, **40**, 609 (1973).
(7) A. M. Horgan and D. A. King, *Surf. Sci.*, **23**, 259 (1970).
(8) G. W. Simmons and D. J. Dwyer, *Surf. Sci.*, **48**, 373 (1975).
(9) J. S. Valentine, *Chem. Rev.*, **73** (3), 235 (1973).
(10) J. B. R. Dunn, D. F. Shriver, and I. M. Klotz, *Biochemistry*, **14**, 2689 (1975).
(11) J. P. Collman, R. R. Gange, C. A. Reed, T. R. Halbert, G. Lang, and W. T. Robinson, *J. Am. Chem. Soc.*, **97**, 1427 (1975).
(12) W. S. Caughey, C. H. Barlow, J. C. Maxwell, J. A. Volpe, and W. J. Wallace, *Ann. N.Y. Acad. Sci.*, **244**, 1 (1975).
(13) D. M. Kurtz, Jr., D. F. Shriver, and I. M. Klotz, *J. Am. Chem. Soc.*, **98**, 5033 (1976).
(14) A. Dedieu, M. M. Rohmer, and A. Veillard, *J. Am. Chem. Soc.*, **98**, 3717 (1976).
(15) W. A. Goddard, III, and B. D. Olafson, *Proc. Natl. Acad. Sci. U.S.A.*, **72**, 2335 (1975).
(16) M. Zerner, M. Gouterman, and H. Kobayashi, *Theor. Chim. Acta*, **6**, 363 (1966).
(17) R. F. Kirchner and G. H. Loew, *J. Am. Chem. Soc.*, **99**, 4639 (1977).
(18) A. B. P. Lever, G. A. Ozin, and H. B. Gray, *Inorg. Chem.*, **19**, 1824 (1980).
(19) L. Vaska, *Acc. Chem. Res.*, **9**, 175 (1976).
(20) (a) S. Abramowitz, N. Acquista, and I. W. Levin, *Chem. Phys. Lett.*, **50**, 423 (1977); (b) R. F. Barrow and M. Senior, *Nature (London)*, **223**, 1359 (1969).
(21) R. C. Baetzold, *Adv. Catal.*, **25**, 1 (1976).
(22) G. Blyholder, *Comput. Chem. Educ. Res., Proc. Int. Conf., 3rd*, 189 (1977).
(23) A. D. Bacon and M. C. Zerner, *Theor. Chim. Acta*, **53**, 21 (1979).
(24) G. Klopman and R. C. Evans, *Mod. Theor. Chem.*, **7**, 29 (1977).
(25) R. C. Bingham, M. J. S. Dewar, and O. H. Lo, *J. Am. Chem. Soc.*, **97**, 1285, 1294, 1302, 1307 (1975).
(26) M. C. Flanigan, A. Komornicki, and J. W. McIver, Jr., *Mod. Theor. Chem.*, **8**, 1 (1977).

Table I. Parameters for Iron

	orbital exponents[29]			core parameters, eV[30]		
	s	p	d	W_{ss}	W_{pp}	W_{dd}
	1.3583	1.3585	3.7266	-102.13	-74.57	-127.29

	Slater–Condon parameters, eV[30]					
	(3d, 3d)	(3d, 4s)	(3d, 4p)	(4s, 4s)	(4s, 4p)	(4p, 4p)
F^0	17.999 88	13.749 57	10.076 12	12.484 27	9.483 61	8.280 22
F^2	8.414 23		0.676 93		2.452 89	
F^4	5.106 33					
G^1			0.250 98		2.201 64	
G^2		1.384 66				
G^3			0.165 81			

Bond Parameters for Fe–O Bonds

$\beta_s = 2.533$ $K_p = 0.35$ $\alpha = 2.991$

where γ is a diatomic electron repulsion integral and α is a constant to be determined.

The computer program used is based on QCPE program 290 by Rinaldi as modified by Schmidling[27] to incorporate MINDO/3 and vibrational calculations. The Rinaldi program has automatic geometry optimization using analytically calculated gradients. We modified the Schmidling version to handle transition metals and use symmetry and selective molecular orbital occupancy. In one option any number of molecular orbitals from the Hückel stage used to obtain an initial density matrix may be completely or partially filled (provided the total number of electrons is correct for the multiplicity selected). After the first electronic cycle calculation with this specified filling, the molecular orbitals with the lowest one-electron eigenvalues will be given in subsequent cycles one electron each unless the top orbital is degenerate, in which case the degenerate orbitals are partly filled with the same fractional filling so that symmetry is preserved and the total electron count is correct. In another option[28] designed by John Head the irreducible representation of each Hückel molecular orbital is enumerated and stored. On subsequent runs the irreducible representations to be occupied by electrons may be specified for the first SCF interaction. Because the SCF procedure usually produces a large splitting between the occupied and unoccupied orbitals, the specified orbitals will continue to be occupied. Atomic parameters for iron together with references to their origin and bonding parameters for Fe–O bonds are given in Table I.

3. Results and Discussion

The results will be presented and discussed in the following three subsections: 3.1, Bonding in FeO, FeO⁺, and FeO⁻; 3.2, Side-Bonded and Linear FeO₂, which includes neutral and charged species; 3.3, Dissociation of Coordinated O_2.

3.1. Bonding in FeO, FeO⁺, and FeO⁻. The results of calculations for a variety of configurations for FeO are given in Table II. The bonding and charge distribution properties calculated for the lowest state of FeO ($^5\Delta$) are given in Table III. The ground state for FeO is the subject of considerable controversy[31-34] and has not been definitely established. The only ab initio calculation[32] did not arrive at a conclusion as to the ground state but did conclude that it was not $^5\Sigma^+$.

(27) D. Schmidling, private communication.
(28) J. D. Head, G. Blyholder, and F. Ruette, *J. Comput. Phys.*, in press.
(29) E. Clementi and D. L. Raimondi, *J. Chem. Phys.*, **38**, 2686 (1963).
(30) G. de Brouckere, *Theor. Chim. Acta*, **19**, 310 (1970).
(31) D. W. Green, G. T. Reedy, and J. G. Kay, *J. Mol. Spectros.*, **78**, 257 (1979).
(32) P. S. Bagus and H. J. T. Preston, *J. Chem. Phys.*, **59**, 2986 (1973).
(33) T. C. DeVore and T. N. Gallaher, *J. Chem. Phys.*, **70**, 4429 (1979).
(34) P. C. Engelking and W. C. Lineberger, *J. Chem. Phys.*, **66**, 5054 (1977).
(35) "Selected Constants, Spectroscopic Data Relative to Diatomic Molecules", B. Rosen, Ed., Pergamon Press, Elmsford, N.Y., 1970.

Table II. FeO

multiplicity	config'n	binding energy, kcal/mol	equilibrium dist, A	charge on O atom
7	α set-$\sigma\sigma\pi^2\delta^2\pi^2\sigma\sigma$ β set-$\sigma\sigma\pi^2$	-48.7	1.71	0.02-
5	α set-$\sigma\sigma\pi^2\delta^2\pi^2\sigma$ β set-$\sigma\sigma\pi^2\delta$	-124.3	1.70	0.20-
5	α set-$\sigma\sigma\pi^2\delta^2\pi^2\sigma$ β set-$\sigma\sigma\pi^2\sigma$	-89.9 -89.9	1.80 1.80	0.36- 0.36-
5	α set-$\sigma\sigma\pi^2\delta^2\pi^2\sigma$ β set-$\sigma\sigma\pi\delta\sigma$	-85.7	2.03	0.27-
5	α set-$\sigma\sigma\pi^2\delta^2\pi^2\sigma$ β set-$\sigma\sigma\pi^2\pi$	-57.1	2.01	0.25-
3	α set-$\sigma\sigma\pi^2\delta^2\pi^2$ β set-$\sigma\sigma\pi^2\pi^2$	-106.6	1.64	0.08-
3	α set-$\sigma\sigma\pi^2\pi^2\delta^2$ β set-$\sigma\sigma\pi^2\delta^2$	-104.6	1.56	0.07-
1	α set-$\sigma\sigma\pi^2\delta^2\sigma$ β set-$\sigma\sigma\pi^2\delta^2\sigma$	+7.4	1.73	0.25-
1	α set-$\sigma\sigma\pi^2\pi^2\sigma$ β set-$\sigma\sigma\pi^2\pi^2\sigma$	+95.8	1.82	0.38-

Table III. FeO ($^5\Delta$) Properties

Fe orbital occupancies			Mulliken bond order	
s	p	d	sp-sp	sp-d
0.67	0.73	6.40	1.05	0.11

	calcd	exptl[35,31]
binding energy, kcal/mol	-124	-90
bond length, A	1.70	1.63
vib freq, cm⁻¹	1013	880

Semiempirical calculations such as those here are not the most appropriate way to determine the ground state of FeO, but they do offer some insight. The existence of a large number of low-lying states shown in Table II suggests that an accurate calculation of the ground state of FeO will require configuration interaction. The substantial 4p orbital occupancy in Table III suggests that the choice of 4p orbital exponents and coefficients will considerably affect any ab initio calculation. The Mulliken bond orders in Table III indicate that the bonding is primarily due to iron 4s and 4p orbitals with relatively little contribution from the 3d orbitals.

The charged species FeO⁺ and FeO⁻ have received very little attention, with but one paper for FeO⁻ having appeared.[34] Energies, bond lengths, and atomic charges for a variety of electronic configurations of FeO⁺ and FeO⁻ are presented in Table IV. A comparison of the properties of the calculated ground states of the neutral and charged FeO species is given in Table V. The binding energies are for the dissociation reactions FeO⁺ → Fe⁺ + O and FeO⁻ → Fe + O⁻, which assume that the odd electron goes with the most electronegative element. The normalized vibrational frequencies, which are

Table IV. FeO⁺ and FeO⁻

multiplicity	config	energy rel to neutral atoms, kcal/mol	equilibrium dist, Å	charge on Fe	charge on O
		FeO⁺			
6	α set-σσπ²δ²π²σ β set-σσπ²	+118.8	1.66	0.73+	0.27+
4	α set-σσπ²δ²π² β set-σσπ²δ	+81.9	1.50	0.49+	0.51+
4	α set-σσπ²δ²π² β set-σσπ²π	+118.8	1.61	0.65+	0.35+
4	α set-σσπ²δ²π² β set-σσπ²σ	+135.2	1.79	0.86+	0.14+
2	α set-σσπ²δ²σ β set-σσπ²δ²	+132.9	1.26	0.13+	1.13+
2	α set-σσπ²δ²σ β set-σσπ²π²	+150	1.92	0.98+	0.02+
2	α set-σσπ²π²σ β set-σσπ²δ²	+192.8	1.71	0.73+	0.27+
2	α set-σσπ²π²σ β set-σσπ²π²	+220	1.76	0.84-	0.16+
		FeO⁻			
6	α set-σσπ²δ²π²σσ β set-σσπ²δ	-97.2	1.79	0.47-	0.53-
6	α set-σσπ²δ²π²σσ β set-σσπ²π	-91.2	1.82	0.44-	0.56-
6	α set-σσπ²δ²π²σσ β set-σσπ²σ	-80.6	1.88	0.36-	0.64-
4	α set-σσπ²δ²π²σ β set-σσπ²π²	-100.3	1.83	0.34-	0.66-
4	α set-σσπ²δ²π²σ β set-σσπ²δ²	-53.5	1.59	0.81-	0.19-
2	α set-σσπ²δ²π² β set-σσπ²π²σ	-59.8	1.69	0.67-	0.33-
2	α set-σσπ²δ²π² β set-σσπ²δ²σ	-43.9	1.64	0.74-	0.26-

normalized to the experimental FeO frequency, show excellent agreement between the normalized and experimental FeO⁻ frequencies.

In simple molecular orbital models it is often assumed that in forming positive or negative ions, electrons can be removed or added to rigid molecular orbitals for the neutral species. It is interesting to see to what extent this assumption is followed in forming FeO⁺ and FeO⁻ (see Table V). The assumption works fairly well for FeO⁺. The highest energy orbital for the ground state FeO is a σ molecular orbital that is antibonding. The positive ion would be expected to be formed by removing the electron from this σ orbital, and indeed the lowest energy state for FeO⁺ has this configuration. Since an electron is removed from an antibonding orbital, the bond length would be expected to decrease, the vibrational frequency to increase, and the bond energy to increase. The first two predictions are borne out by the calculations, but the last one is not. In the formation of FeO⁻ it is expected that the extra electron would fill the half-filled δ orbital in the β set, with little change in properties since this is a nonbonding orbital. However, the calculations show the lowest state of FeO⁻ has the charge reorganized to leave this δ orbital empty and a π* orbital filled with the changes in properties expected from filling a slightly

antibonding molecular orbital. The reason the electron does not go into the δ orbital is evident in considering the calculation of the last multiplicity 4 state for FeO⁻ in Table IV. When the electron is put into the δ orbital, it is put entirely on the iron atom since the δ orbital does not interact with any oxygen orbitals. Since the iron atom is less electronegative than oxygen, this is not the best place for it, and so by the movement into a π* orbital it is delocalized onto the more electronegative oxygen atom where it is more stable. Thus the rigid molecular orbital model does have some predictive value, but detailed calculations do reveal variations.

3.2 Side-Bonded and Linear FeO₂. The results for a number of different configurations for side-bonded FeO₂ are given in Table VI. The lowest energy obtained was for an intermediate-spin, multiplicity 5, state. It may be seen from Table VI that there are many states with energies quite close to the lowest energy in this single Slater determinant approximation. This suggests that configuration interaction could be important in determining exact energies and their relative positions for different configurations as has been found in other transition-metal complexes.[23] MINDO/3 gives a rather high vibrational frequency for O₂. The vibrational frequency calculated for the O–O stretch in FeO₂ is 1583 cm⁻¹, which is 73% of the MINDO/3 frequency for O₂. The experimental frequency of the O–O stretch in matrix-isolated FeO₂ is 61% of the experimental O₂ stretching frequency, which gives reasonable agreement between calculation and experiment.

Consideration of the calculated molecular orbitals for side-bonded FeO₂ leads to a consistent molecular orbital (MO) picture for the bonding in free O₂ and bound O₂. In free O₂ there are four electrons in π-bonding MO's and two in π* antibonding MO's. The MO's for side-bonded FeO₂ show four electrons in orbitals that are largely π bonding for the bound O₂ and three electrons in orbitals that are π* for the bound O₂. This extra electron in a π* MO results in a substantial reduction in the O–O bond order as may be seen in Table VII. The bonding between Fe and O₂ occurs largely in two MO's one of which has a bonding interaction between the 4s orbital of Fe and the 2s orbital of each oxygen atom. The other bonding MO has an interaction between the 4s orbital of Fe and the p_x orbital of each O atom. The contributions of the oxygen 2s and 2p orbitals to the bonding are about equal. The bond between Fe and O₂ may be qualitatively described as being due to 3-center bonds. The oxygen 2s orbitals with the 4s orbital of Fe from a 3-center bond, and a π MO of O₂ combines with the 4s orbital of Fe to form another multicenter bond.

The results for a number of configurations for end-bonded Fe–O–O are given in Table VIII. The lowest energy state obtained has an intermediate spin of multiplicity 3. Again there are a number of configurations with energies quite close to the lowest energy. The lowest energy states have a linear geometry. These calculations have the end-bonded geometry at a slightly lower energy than the side-bonded geometry, whereas the matrix-isolation spectra indicate that the side-bonded state is more stable. This inversion may be a result of not using configuration interaction in these calculations. Later it will be shown that these calculations give a trend in relative stability for the two geometries as the charge on the

Table V. Properties of FeO, FeO⁺, and FeO⁻

	config	binding energy, kcal/mol	bond length, Å	ν(calcd), cm⁻¹	(880/1013)ν	ν(exptl)
FeO	α set-σ²π²δ²π*²σ* β set-σ²π²δ	-124.3	1.70	1013	880	880
FeO⁺	α set-σ²π²δ²π*² β set-σ²π²δ	-100.3	1.50	1285	1116	
FeO⁻	α set-σ²π²δ²π*²σ β set-σ²π²π*²	-66.5	1.83	861	748	740 ± 60

Table VI. Side-Bonded FeO_2

multiplicity	config^a	energy of atomization, kcal/mol	equilibrium dist, Å		charge on Fe
			Fe–O	O–O	
7	$(a_1)^4(b_2)(b_1)^2 \mid (a_2)^2(a_1)(b_2)(b_1)^2$	−39.5	2.25	1.43	0.28+
7	$(a_1)^3(b_2)^2(b_1)^2 \mid (a_1)^2(a_2)^2(b_1)^2$	−34.0	2.25	1.43	0.27+
7	$(a_1)^3(b_2)(b_1)^2(a_2) \mid (a_1)^2(a_2)(b_2)(b_1)^2$	−32.6	2.25	1.43	0.28+
7	$(a)^3 b_2(b_1)^3 \mid (a_1)^2(a_2)^2(b_2)(b_1)$	−22.9	2.25	1.43	0.22+
5*	$(a_1)^4(b_1)^2(b_2)^2 \mid (a_2)^2(b_1)(a_1)$	−111.9	2.27	1.34	0.28+
5	$(a_1)^5(b_1)^2(b_2) \mid (a_2)^2(b_1)(b_2)$	−111.2	2.27	1.34	0.29+
5	$(a_1)^4(b_1)^2(b_2)(a_2) \mid (b_1)(a_2)(b_2)(a_1)$	−108.0	2.29	1.34	0.33+
5	$(a_1)^3(b_1)^2(b_2)(a_2)^2 \mid (b_1)(a_1)^2(b_2)$	−101.0	2.28	1.34	0.33+
5	$(a_1)^3(b_1)^2(b_2)^2(a_2) \mid (b_1)(a_1)^2(a_2)$	−102.0	2.28	1.34	0.33+
5	$(a_1)^4(b_1)^2(b_2)^2 \mid (a_2)^2(b_2)(a_1)$	−110.8	2.27	1.34	0.28+
5	$(a_1)^3(b_1)^3(b_2)(a_2) \mid (a_1)^2(a_2)(b_2)$	−54.6	2.11	1.49	0.54+
3	$(b_1)^2(a_2)(a_1)^4(b_2)^2 \mid (a_1)(a_2)$	−108.9	2.29	1.34	0.33+
3	$(b_2)(b_1)^2(a_2)^2(a_1)^4 \mid (b_2)(a_1)$	−107.1	2.29	1.34	0.33+
3	$(a_1)^5(a_2)(b_2)^2(b_1) \mid (b_1)^2$	−41.8	2.31	1.34	0.34+
3	$(b_1)^3(a_2)(a_1)^3(b_2)^2 \mid (a_1)(a_2)$	−5.5	2.06	1.49	0.48+
1	$(b_1)^3(a_1)^5(b_2)^2$	−5.8	5	1.21	0.00+
1	$(b_1)^2(a_1)^4(b_2)^2(a_2)^2$	−2.6	2.04	1.45	0.38+
1	$(b_1)^3(a_1)^4(b_2)^2(a_2)$	+22.3	2.06	1.49	0.48+

^{a} C_{2v} symmetry notation. All orbitals listed are in the α set; orbitals up to the vertical line are in the β set.

Table VII. Bond Orders and Vibrational Frequencies for Free and Bound O_2

	O–O bond order	freq, cm^{-1}
free O_2	1.20	2157
side-bonded FeO_2 (lowest state)	0.80	1583
end-bonded Fe–O–O (lowest state)	0.94	1848
side-bonded FeO_2^+ (lowest state)	1.12	
side-bonded FeO_2^{2+} (lowest state)	1.09	
end-bonded Fe–O–O^{2+} (lowest state)	1.23	
side-bonded FeO_2^- (lowest state)	0.52	

Table VIII. End-Bonded Fe–O–O (Linear)

multiplicity	config^a	energy of atomization, kcal/mol	equilibrium dist, Å		charge on Fe
			Fe–O	O–O	
7	$(a')^4(a'')^3 \mid (a')^5(a'')^1$	−117.7	1.97	1.27	0.13+
7	$(a')^6(a'')^1 \mid (a')^3(a'')^3$	−117.0	1.97	1.27	0.14+
7	$(a')^5(a'')^2 \mid (a')^4(a'')^2$	−60	1.7	1.5	0.25+
5	$(a')^6(a'')^2 \mid (a')^2(a'')^2$	−155.2	1.98	1.27	0.21+
5	$(a')^5(a'')^3 \mid (a')^3(a'')^1$	−155.1	1.98	1.27	0.21+
3*	$(a')^7(a'')^2 \mid (a')^1(a'')^1$	−156.1	1.98	1.27	0.21+
3	$(a')^5(a'')^4 \mid (a')^2$	−147.2	1.99	1.27	0.22+
1	$(a')^6(a'')^4$	−30	1.8	1.3	0.26+

^{a} C_s symmetry notation. All orbitals listed are in the α set; orbitals up to the vertical line are in the β set.
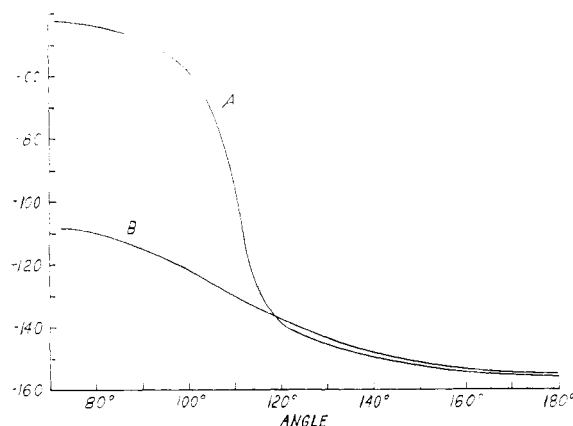

Figure 1. Variation of energy (kcal/mol) with bond angle for Fe–O–O: curve A, lowest energy configuration of multiplicity 3; curve B, lowest energy configuration of multiplicity 5.

iron is changed that is in accord with experiment.

The variation in energy with the Fe–O–O bond angle is shown in Figure 1 for the two lowest configurations for end-bonded Fe–O–O. The energies were obtained by fixing the bond angle and allowing the bond lengths to vary until an energy minimum was reached. No minimum at any place other than the linear shape is found. Since end-bonded O_2 in iron complexes is found to be bent, the results here suggest that the orbital interactions with the ligands other than O_2 play a role in determining the Fe–O–O geometry in dioxygen complexes.

In all cases of either side-bonded or end-bonded O_2 the charge on the bound O_2 is negative in accord with experiment.[18] For side-bonded O_2 the charge on the O_2 in the lowest energy state is 0.28− while for end-bonded O_2 it is 0.21−.

For the investigation of the effect of iron atom charge on the relative stability of side-bonded vs. end-bonded O_2 calculations were made for FeO_2 species with a 2+ charge. The results in Table IX show the end-bonded O_2 for Fe^{2+} to be about 60 kcal/mol more stable than the side-bonded species,

which is in accord with O_2 bonded to Fe(II) and Fe(III) in iron porphyrins being experimentally found to be end-bonded. Tables VI and VIII indicate that the end-bonded O_2 is about 45 kcal/mol more stable than the side-bonded O_2 for neutral iron atoms so that the trend in the effect of charge is for increasing positive charge to make the end-bonded O_2 more stable with respect to the side-bonded O_2. This trend is in accord with the experimental trend established by the more stable species being side bonded in matrix FeO_2 but end bonded for $Fe^{II}O_2$ in iron porphyrins.

3.3 Dissociation of Coordinated O_2. In the catalytic oxidation of organic compounds and the oxidation of metals the first step is often assumed to be the dissociation of O_2 into individual coordinated oxygen atoms or at least the activation, i.e., the weakening, of the O–O bond by coordination with a metal atom. These processes will be examined in this section for interaction with a single iron atom. We shall consider first the change in bond order for the O—O bond caused by coordination with an iron atom, then the structure of O—Fe—O, and finally the energy of an FeO_2 complex as the O—O bond is broken.

The calculated bond orders and vibrational frequencies for free, side-bonded and end-bonded O_2 are given in Table VII. Both the bond orders and the vibrational frequencies indicate that coordination weakens the O–O bond and so activates the O_2 molecule for reaction.

The results of calculations for OFeO, OFeO$^+$, and OFeO$^-$ are given in Table X. In geometry optimization calculations

Table IX. Energies for Side-Bonded FeO$_2$$^{2+}$ and End-Bonded Fe-O-O^{2+}

multiplicity	config^a	energy wrt neutral atoms, kcal/mol	equilibrium dist, Å Fe–O	equilibrium dist, Å O–O	charge on Fe
		Side-Bonded FeO$_2$$^{2+}$			
7*	$(a_1)^3(b_1)^2(b_2)^1 |(a_2)^2(a_1)^2(b_1)(b_2)$	+450.8	2.34	1.24	1.31+
7	$(a_1)^3(b_1)^1(b_2)^1(a_2)^1 |(a_2)^1(a_1)^2(b_1)^2b_2$	+451.7	2.35	1.24	1.31+
5	$(a_1)^3(b_1)^2(a_2)(b_2) |(a_1)^2(a_2)(b_2)$	+459	2.33	1.24	1.29+
5	$(a_1)^3(b_1)^2(a_2)(b_2) |(a_1)(a_2)(b_1)(b_2)$	+510	2.34	1.24	1.30+
5	$(a_1)^3(b_1)^2(a_2)(b_2) |(a_1)^2(b_1)(b_2)$	+531	2.34	1.24	1.31+
5	$(a_1)^3(b_1)^2(a_2)(b_2) |(a_1)^2(b_1)(b_2)$	+475	2.30	1.23	1.25+
3	$(a_1)^4(b_1)^2(a_2)(b_2) |(a_2)(b_2)$	+522	2.36	1.24	1.32+
3	$(a_1)^3(b_1)^2(a_2)^2(b_2) |(a_1)(b_2)$	+539	2.36	1.24	1.32+
3	$(a_1)^3(b_1)^2(a_2)(b_2) |(a_1)(a_2)$	+518	2.31	1.24	1.27+
3	$(a_1)^3(b_1)^3(a_2)(b_2) |(a_1)(a_2)$	+663	2.31	1.28	1.27+
1	$(a_1)^4(b_1)^2(b_2)^2(a_2)^2$	+568	2.37	1.24	1.33+
1	$(a_1)^4(b_1)^2(b_2)^2(a_2)^1$	+754	1.77	1.82	0.84+
1	$(a_1)^4(b_1)^3(b_2)(a_2)$	+566	2.33	1.23	1.29+
1	$(a_1)^3(b_1)^3(b_2)^2(a_2)^2$	+566	2.34	1.24	1.31+
		End-Bonded Fe-O-O^{2+} (Linear)^b			
7*	$(a')^5(a'')^1 |(a')^3(a'')^3$	+390	2.06	1.19	1.26+
7	$(a')^4(a'')^2 |(a')^4(a'')^2$	+390	2.06	1.19	1.25+
5	$(a')^5(a'')^2 |(a')^2(a'')^2$	+460	2.0	1.1	0.62+
3	$(a')^5(a'')^3 |(a')^2$	+546	1.28	2.29	0.69+
1	$(a')^7(a'')^2$	+520	2.1	1.2	1.28+

^{a} C_{2v} symmetry notation. All orbitals listed are in the α set; orbitals up to the vertical line are in the β set. ^{b} C_s symmetry notation.
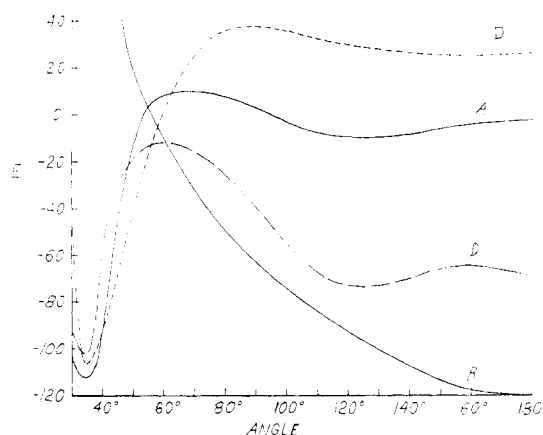

Figure 2. O–Fe–O energy (kcal/mol) as a function of bond angle: curve A, configuration from line 5 of Table VI; curve B, configuration from line 9 of Table VI; curve C, configuration from line 7 of Table VI; curve D, configuration from line 1 of Table X.

Figure 3. Energy (kcal/mol) of O–Fe–O$^+$ as a function of bond angle: curve A, lowest energy configuration of multiplicity 6; curve B, lowest energy configuration of multiplicity 4.

Figure 4. Energy (kcal/mol) of O–Fe–O$^-$ as a function of bond angle: curve A, lowest energy configuration of multiplicity 4; curve B, lowest energy configuration of multiplicity 6.

the lowest energy states for these molecules were found to be linear except in the one case noted in the table. For the comparison of energies before and after bond breaking the results of calculations for side-bonded FeO$_2$$^+$ and FeO$_2$$^-$ are given in Table XI. In the comparison of the energies of side-bonded O$_2$ with linear OFeO it is seen that with a 1+ charge the side-bonded structure with the O–O bond intact is more stable by about 88 kcal/mol than the open structure with the O–O bond broken. For the neutral species the open structure is slightly (8 kcal/mol) more stable while for the negatively charged species the open structure with the O–O bond broken is much more stable (about 68 kcal/mol) than the side-bonded structure. Thus in biological systems using hemoglobin to transport O$_2$ there should be no tendency for the O$_2$ to dissociate while coordinated to Fe(II) or Fe(III).

For the examination of the dissociation process, the energy as a function of the O–Fe–O bond angle was calculated for various orbital occupancies and is shown for neutral FeO$_2$ in Figure 2. The energies were calculated as energy minima as the FeO distance was varied at a fixed bond angle. Thus a minimum-energy path is calculated. The curves in Figure 2 indicate that an activation energy at 0 K of at least 100
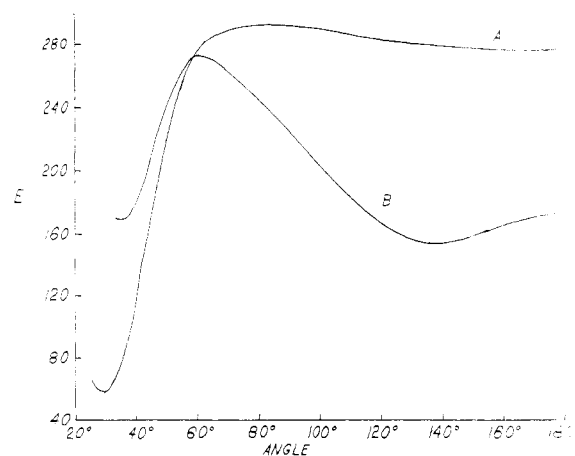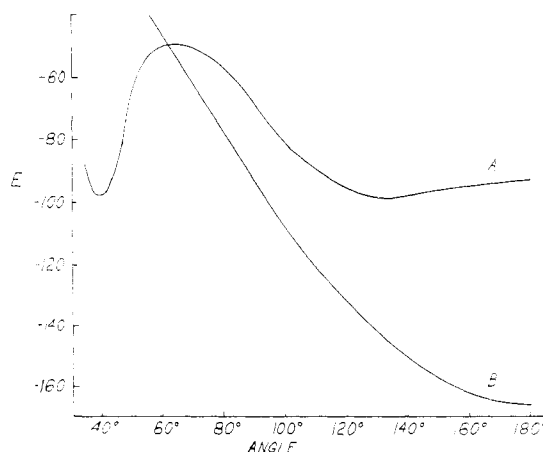
kcal/mol would be required to break the O–O bond of coordinated O$_2$. Note also that the most stable side-bonded and open species are in different spin states. These results suggest

Table X. Energies for O-Fe-O Groups (Linear)

multiplicity	config[a]	energy wrt neutral atoms, kcal/mol	Fe-O equilibrium dist, Å	charge on Fe
	O-Fe-O			
7*	$(a_1)^2(b_1)^3(a_2)(b_1)\|(a_1)^3(a_2)(b_1)(b_2)$	−119.7	2.02	0.46+
7	$(a_1)^3(b_1)^2(a_2)(b_2)\|(a_1)^2(b_1)^2(a_2)(b_2)$	−116.7	2.04	0.47+
7	$(a_1)^3(b_1)^3(b_2)\|(a_1)^2(b_1)(a_2)^2(b_2)$	−76.2	1.94	0.10+
5	$(a_1)^3(b_1)^3(a_2)(b_2)\|(a_1)(a_2)(b_1)(b_2)$	−72.6	1.68	0.07+
5	$(a_1)^3(b_1)^3(a_2)(b_2)\|(a_1)^2(b_1)(b_2)$	−68.9	1.90	0.10+
5	$(a_1)^3(b_1)^3(a_2)(b_2)\|(a_1)^2(b_1)(a_2)$	+1	1.92	0.08+
3	$(a_1)^3(b_1)^3(a_2)^2(b_2)\|(a_1)(b_2)$	−116.2	2.04	0.50+
3	$(a_1)^4(b_1)^3(a_2)^1(b_2)\|(a_2)(b_2)$	−103.1	1.73	0.01−
3	$(a_1)^3(b_1)^3(a_2)(b_2)^2\|(a_1)^2$	−82.7	1.92	0.05+
3	$(a_1)^4(b_1)^3(a_2)(b_2)\|(a_1)(b_2)$	−82.7	1.92	0.05+
3	$(a_1)^3(b_1)^4(a_3)(b_2)\|(a_1)(b_2)$	−61.0	1.78	0.07+
1	$(a_1)^3(b_1)^4(a_2)(b_2)^2$	−9.1	1.70	0.08−
	O-Fe-O⁺			
8	$(a_1)^2(b_1)^2(b_2)(a_2)\|(a_1)^3(b_1)^2(a_2)(b_2)$	+145	2.0	0.52+
6	$(a_1)^3(b_1)^2(a_2)(b_2)\|(a_1)(b_1)^2(a_2)(b_2)$	+171.9	2.01	0.50+
6	$(a_1)^3(b_1)^3(b_2)\|(a_1)^2(b_1)(a_2)^2$	+174.5	2.18	0.20+
6	$(a_1)^3(b_1)^3(b_2)\|(a_1)(b_1)(a_2)^2(b_2)$	+184.0	2.04	0.51+
6	$(a_1)^3(b_1)^3(b_2)\|(a_1)^2(b_2)(a_2)^2$	+219	1.92	0.31+
6	$(a_1)^3(b_1)^3(b_2)\|(a_1)^2(b_1)(a_2)(b_2)$	+234	1.93	0.32+
4[b]	$(a_1)^3(b_1)^3(a_2)(b_2)\|(a_1)(a_2)(b_2)$	+153.7	1.59	0.07+
4	$(a_1)^3(b_1)^3(a_2)(b_2)\|(a_1)(b_1)(a_2)$	+182.8	1.95	0.37+
4	$(a_1)^3(b_1)^3(a_2)(b_2)\|(a_1)(b_1)(b_2)$	+186	1.61	0.02+
	O-Fe-O⁻			
6*	$(a_1)^3(b_1)^3(b_2)(a_2)\|(a_1)^2(a_2)(b_1)(b_2)$	−166.0	1.94	0.03−
6	$(a_1)^3(b_1)^3(b_2)^2\|(a_1)(a_2)^2(b_1)$	−161.3	1.96	0.03−
4	$(a_1)^3(b_1)^3(a_2)(b_2)^2\|(a_1)(b_1)(a_2)$	−111.5	2.11	0.10−
4	$(a_1)^4(b_1)^3(a_2)(b_2)\|(b_1)(b_2)(a_1)$	−111.5	2.11	0.10−
4	$(a_1)^3(b_1)^3(a_2)^2(b_2)\|(a_1)(b_1)(b_2)$	−132.7	1.79	0.04−
4	$(a_1)^3(b_1)^4(a_2)(b_2)\|(a_1)(b_2)(a_2)$	−132.7	1.79	0.04−

[a] C_{2v} symmetry notation. All orbitals listed are in the α set; orbitals up to the vertical line are in the β set. [b] Equilibrium bond angles is 138°.

Table XI. Side-Bonded FeO_2^+ and FeO_2^-

multiplicity	config	energy wrt neutral atoms, kcal/mol	equilibrium dist, Å Fe-O	equilibrium dist, Å O-O	charge on Fe
	FeO_2^+				
8	$(a_1)^3(b_1)(b_2)^2\|(a_1)^2(b_1)^3(a_2)^2$	+162.8	2.36	1.24	0.47+
6*	$(a_1)^4(b_1)(b_2)^2\|(a_1)(b_1)^2(a_2)^2$	+57.5	2.42	1.23	0.55+
4	$(a_1)^3(b_1)^2(b_2)^2(a_2)\|(a_1)^2(b_1)$	+72.6	2.40	1.23	0.55+
	FeO_2^-				
6	$(a_1)^4(b_1)^2(a_2)(b_2)\|(a_1)(b_1)^2(a_2)(b_2)$	−44.4	2.38	1.34	0.47−
4*	$(a_1)^4(b_1)^2(a_2)(b_2)^2\|(a_1)(b_1)(a_2)$	−97.8	2.20	1.49	0.03−

that O_2 dissociation on a single metal atom is not a very likely process.

It has been suggested that the negative charge buildup predicted by Hückel calculations for metal atoms at edge positions in crystallites would facilitate the dissociation of O_2.[36] The energies as a function of bond angle for FeO_2^+ and FeO_2^- are given in Figures 3 and 4. Again this is a minumum-energy path calculated by varying the Fe–O distance at a fixed bond angle. These results show a very high activation energy for O–O bond breaking in FeO_2^+ but a considerably reduced activation energy (about 45 kcal/mol at 0 K) for O–O bond breaking in FeO_2^-. This result supports the idea that negatively charged atoms on a surface would facilitate the dissociation of O_2 on a metal surface. The reality of negative charges on step atoms of a surface is very much in question since Hückel theory often produces unrealistic charge separations due to its neglect of explicit electron repulsion terms. Even though the barrier to O_2 dissociation is reduced for a negatively charged Fe atom, the barrier of 45 kcal/mol is still quite large,

which leads to the likelihood that O_2 dissociation on an Fe surface does not occur by interaction of O_2 with a single surface atom but rather occurs by interaction with several metal atoms. The existence of a potential well for undissociated O_2 interacting with an iron atom supports the proposal[7,8] of molecularly adsorbed O_2 as a precursor state in metal oxidation.

4. Conclusions

A modified MINDO procedure works well to discuss iron-oxygen interactions. The iron orbitals that contribute most to bonding in FeO are the 4s and 4p orbitals with relatively little contribution from the 3d orbitals. The molecular orbital model used gave a good account of the vibrational frequencies in the various charged species. A rigid molecular orbital model for FeO^+ and FeO^- derived from the MO's for FeO was found to have some predictive value, but explicit calculations for FeO^+ and FeO^- reveal variations from the predictions. Comparison of calculations for side-bonded and linear FeO_2 show that as positive charge on the Fe atom is increased, the linear structure is favored. Back-donation of charge from the Fe atom into π^* orbitals on oxygen weakens the O–O bond

(36) A. B. Anderson and R. Hoffmann, *J. Chem. Phys.*, **61**, 4545 (1974).

in coordinated O_2. No activation barrier is found for rotation of the O–O group from the side-bonded to the linear position. The most stable bond angle in O–Fe–O is calculated to be 180°. For dissociation of the O–O bond in side-bonded FeO_2 to form O–Fe–O, an activation energy of 100 kcal/mol is calculated. Negative charge on the complex decreases the activation energy while positive charge increases it. Thus single iron atoms are a poor catalyst for dissociation of O_2, which suggests that dissociative adsorption of O_2 on iron surfaces most likely occurs on a site where the O_2 interacts with several iron atoms.

Appendix

In order to demonstrate that the procedure can handle a wide range of compounds, we have done calculations for FeH, FeH_4, Fe_2, Fe_6, $Fe(CO)_5$, FeO, FeO_2, OFeO, NiH, NiH_2, Ni_2H_2, NiO, Ni_2, Ni_6, and $Ni(CO)_4$. While some of these calculations are still in preliminary stages, it has been possible to find satisfactory parameters in all cases even though the final optimized parameters have not been established for all these compounds. Parameters selected to give FeH a bond

energy of 60 kcal/mol at an equilibrium bond length of 1.50 Å produce a calculation for FeH_4 in good agreement with an ab initio calculation by Hood, Pitzer, and Schaefer;[37] i.e., both calculations give a moderately stable $^5T_2(t_2{}^2e^2)$ ground state with a 4p orbital occupancy around 1. Parameters selected to give Fe_2 a bond energy of 30 kcal/mol[38] at an equilibrium bond length of 2.3 Å when used in a Fe_6 cluster calculation indicate a stable cluster with a "d" bandwidth of 3.5 eV, which is similar to 4.0 eV given by our $X\alpha$ calculation. The $Fe(CO)_5$ calculation gives orbital energies that differ by less than 0.5 eV from the principal bands in the experimental[39] photoelectron spectrum of $Fe(CO)_5$. Having verified that the calculational procedure gives reasonable results for a wide variety of transition-metal compounds, this paper has concentrated on iron–oxygen interactions. More details about the procedure are being published.[40]

(37) D. M. Hood, R. M. Pitzer, and H. F. Schaefer III, *J. Chem. Phys.,* **71,** 705 (1979).
(38) S. Lin and A. Kant, *J. Phys. Chem.,* **73,** 2450 (1969).
(39) E. J. Baerends, C. Oudshoorn, and A. Oskam, *J. Electron. Spectrosc. Relat. Phenom.,* **6,** 259 (1975).
(40) G. Blyholder, J. Head, and F. Ruette, *Theor. Chim. Acta,* in press.

Contribution from the Department of Chemistry, University of California, Riverside, California 92521

Redox Chemistry of Metal–Catechol Complexes in Aprotic Media. 4. Synthesis and Characterization of 3,5-Di-*tert*-butylcatecholato Complexes of Vanadium(V), -(IV), and -(III)

PAULA J. BOSSERMAN and DONALD T. SAWYER*

The disodium bis(3,5-di-*tert*-butylcatecholato)methoxyoxovanadate(V), disodium bis(3,5-di-*tert*-butylcatecholato)oxovanadate(IV), disodium dichlorobis(3,5-di-*tert*-butylcatecholato)vanadate(IV), and trisodium tris(3,5-di-*tert*-butylcatecholato)vanadate(III) complexes have been synthesized and isolated. These and related species have been characterized by cyclic voltammetry and controlled-potential electrolysis as well as by UV–visible, IR, proton NMR, and EPR spectroscopy and magnetic susceptibility measurements in aprotic media. The vanadium(III) and -(IV) species are oxidized to vanadium(V) by protic substrates. This is in contrast to the pyrocatechol complexes of vanadium(V), -(IV), and -(III), where vanadium(IV) is the stable oxidation state.

Although vanadium is present in the human body at a level of 0.03 ppm,[1] its biological function is unknown. Vanadium(V) reacts with L-ascorbate to produce vanadium(IV) and dehydroascorbic acid.[2] Vanadium(V) ion also acts as an inhibitor for (Na,K)-ATPase,[3–5] dynein ATPase, and LAD-1.[6] The inhibition is reversed by the addition of catechol (1,2-dihydroxybenzene) or catecholamine. A study of the reaction of norepinephrine (a catecholamine) with vanadium(V) indicates that norepinephrine first complexes and then reduces the vanadium.[7]

The reaction of catechol and its derivatives with various oxidation states of vanadium in protic solvents (water and methanol) has been extensively investigated. Solution studies of vanadium(III) with catechol indicate that the formation of mono, bis, and tris complexes is dependent on pH.[8–10] Vanadium(IV) reacts with catechol to yield $V^{IV}(cat)_3{}^{2-}$, when isolated from solution.[11,12] In solution, the principal species

(1) Ochiai, E. "Bioinorganic Chemistry, An Introduction"; Allyn and Bacon: Boston, 1977.
(2) Kustin, K.; Toppen, D. L. *Inorg. Chem.* **1973,** *12,* 1404.
(3) Hudgins, P. J.; Bond, G. H. *Biochem. Biophys. Res. Commun.* **1977,** *77,* 1024.
(4) Josephson, L.; Cantley, L. C., Jr. *Biochemistry* **1977,** *16,* 4572.
(5) Cantley, L. C., Jr.; Josephson, L.; Warner, R.; Yanagisawa, M.; Lechene, C.; Guidotti, G. *J. Biol. Chem.* **1977,** *252,* 7421.
(6) Gibbons, I. R.; Cosson, M. P.; Evans, J. A.; Gibbons, B. H.; Houck, B.; Martinson, K. H.; Sale, W. S.; Tang, W. Y. *Proc. Natl. Acad. Sci. U.S.A.* **1978,** *75,* 2220.

(7) Cantley, L. C.; Ferguson, J. H.; Kustin, K. *J. Am. Chem. Soc.* **1978,** *100,* 5210.
(8) Ali-Zade, T. D.; Gamizade, G. A.; Agamirova, O. M. *Azerb. Khim. Zh.* **1977,** *31,* 127.
(9) Luneva, N. P.; Nikonova, L. A. *Koord. Khim.* **1979,** *5,* 185.
(10) Nechaeva, N. E.; Lukashevich, M. A., *Elektrodyne Protsessy Elektroosazhdenii Rastvorenii Met.* **1978,** 19.
(11) Henry, R. P.; Mitchell, P. C. H.; Pure, J. E. *J. Chem. Soc. A* **1971,** 3392.